Lab on a Chip

Digital Electrical Impedance Analysis for Single Bacterium Sensing and Antimicrobial Susceptibility Testing

Journal:	*Lab on a Chip*
Manuscript ID	LC-ART-09-2020-000937.R2
Article Type:	Paper
Date Submitted by the Author:	06-Jan-2021

Complete List of Authors:	Scherer, Brian; GE Global Research, Electronics Surrette, Christine; GE Global Research, ETS-MNST Li, Hui; Pennsylvania State University, Torab, Peter; Penn State - Main Campus Kvam, Erik; General Electric - Global Research Center, DIBT Galligan, Craig; General Electric - Global Research Center, MSNT-ETS Go, Steven; GE Global Research Grossmann, Greg; GE Global Research Hammond, Tyler; GE Global Research Johnson, Tammy; GE Global Research St-Pierre, Richard; GE Global Research Nelson, John; General Electric, Life Sciences and Molecular Diagnostics Potyrailo, Radislav; General Electric, Global Research Center; Khire, Tejas; GE Global Research Hsieh, Kuangwen; Johns Hopkins University, Mechanical Engineering Wang, Jeff; The Johns Hopkins University, Mechanical Engineering Wong, Pak Kin; The Pennsylvania University, Biomedical Engineering Puleo, Chris; GE Global Research, ETS-MNST

ARTICLE

Digital Electrical Impedance Analysis for Single Bacterium Sensing and Antimicrobial Susceptibility Testing

Received 00th January 20xx,
Accepted 00th January 20xx

DOI: 10.1039/x0xx00000x

Brian Scherer†[a], Christine Surrette†[a], Hui Li[b], Peter Torab[b], Erik Kvam[a], Craig Galligan[a], Steven Go[a], Greg Grossmann[a], Tyler Hammond[a], Tammy Johnson[a], Richard St-Pierre[a], John R. Nelson[a], Radislav A. Potyrailo[a], Tejas Khire[a], Wen Hsieh[c], Tza-Huei Wang[c], Pak Kin Wong[b], Chris M. Puleo*[a d],

Single-molecule and single-cell analysis techniques have opened new opportunities for characterizing and analyzing heterogeneity within biological samples. These detection methods are often referred to as digital assays because the biological sample is partitioned into many small compartments and each compartment contains a discrete number of targets (e.g. cells). Using digital assays, researchers can precisely detect and quantify individual targets, and this capability has made digital techniques the basis for many modern bioanalytical tools (including digital PCR, single cell RNA sequencing, and digital ELISA). However, digital assays are dominated by optical analysis systems that typically utilize microscopy to analyze partitioned samples. The utility of digital assays may be dramatically enhanced by implementing cost-efficient and portable electrical detection capabilities. Herein, we describe a digital electrical impedance sensing platform that enables direct multiplexed measurement of single cell bacterial cells. We outline our solutions to the challenge of multiplexing impedance sensing across many culture compartments and demonstrate the potential for rapidly differentiating antimicrobial resistant versus susceptible strains of bacteria.

Introduction

Rapid, innovative, and cost-effective tests that detect and characterize drug resistant bacteria remain an unmet need in the global effort to combat multidrug resistant pathogens and promote antimicrobial stewardship.[1-4] To manage infectious diseases, healthcare providers must make timely decisions on antibiotic use based on immediately observable information. Yet, culture-based tests (including broth dilution, antimicrobial gradient or disk diffusion, chromogenic reagents, and automated optical imaging platforms) produce antimicrobial susceptibility test (AST) results in time-frames that are incompatible with desired timely treatment.[5,6] Therefore, the onus for antibiotic stewardship currently falls on technology developers, regulators, and healthcare agencies to develop, test, approve, and promote the use of rapid diagnostics and determine which drug treatment to use in a patient specific manner.[1,3,4,6]

Recently, a new generation of approaches have emerged to rapidly perform AST by utilizing single-cell or single-molecule detection methods (i.e., digital assays).[7-17] These new tests quantify phenotypic or molecular changes associated with the effects of antimicrobial drugs on bacteria after brief (e.g., 0.25 – 2 hour) incubation periods. Rapid AST approaches have utilized digital microscopy,[9,11,16] digital polymerase chain reaction (PCR),[8,14,15,17] single cell cytometry[18], or mass spectrometry[5] to link changes in nucleic acid concentration/protein expression or cellular/microcellular structure to phenotypic AST signatures. Compared to bulk phenotypic tests, digital methods hold promise for accelerated detection of susceptibility; however, these new methods also require complex analytical equipment, cumbersome data processing, or a prohibitively high cost per sample. Importantly, these limitations hinder digital assays for mobile health applications. In contrast, electrical sensing systems are attractive alternatives as they can be built into small portable or hand-held systems and have previously been demonstrated for low-cost applications.[Error! Reference source not found.-21] Electrical and impedance-based sensing has been used to detect the presence of bacteria in bulk formats,[22-26] and can differentiate between viable and non-viable cells.[27] However, despite the portable and cost-effective nature of electrical sensing, the technique has not been extended to digital assays and has not been demonstrated for AST.[Error! Reference source not found.,20] This is due, in part, to the lack of an electrical sensor technology that can handle single cells (e.g., one bacterium/sensor), as prior studies for sensing low bacteria loads are limited to 10-100 bacteria per sensor[23-25]. Another issue is the challenge of

[a.] General Electric Research; Niskayuna, NY, USA. E-mail: chrispuleo@ge.com
[b.] The Pennsylvania State University; Department of Biomedical Engineering, State College, PA, USA.
[c.] The Pennsylvania State University; Department of Mechanical Engineering, State College, PA, USA
[d.] Johns Hopkins University, Department of Mechanical Engineering, Baltimore MD, USA. Johns Hopkins University, Department of Biomedical Engineering, Baltimore MD, USA
† These authors contributed equally to this work.
Electronic Supplementary Information (ESI) available. See DOI: 10.1039/x0xx00000x

multiplexing electrical sensors for robust high-throughput studies that assess different biochemical conditions at once. To be commercially viable, at least hundreds to thousands of bacteria should be analyzed which means a multiplexing solution is needed that enables automated, reliable impedance measurement.

To fill this need, we have designed and implemented a hand-held, multiplexed electrical impedance sensing system in which bacteria are cultured within arrays of nanoliter culture chambers (called nanowells herein) at the single cell level (Fig. 1a). Like optical-based digital assays,[9,11,14] the impedance signal from each nanowell is *not* quantified in a traditional analog manner. Instead, the microfluidic array is loaded with each nanowell containing mostly zero or one bacterium (based on Poisson statistics), and the presence of bacteria – and whether or not they are metabolically active - within each nanowell is assessed based on the percentage change in impedance signal, resulting in a digital readout (i.e., from the analog impedance data, each nanowell is assigned a digital status of either occupied or unoccupied). The concentration of metabolizing bacteria in the sample is then quantified from the fraction of empty nanowells. When doing AST, nanowells with antibiotic can be compared to those without antibiotic and those that are empty (no bacteria) to characterize the bacteria's susceptibility to a specific antibiotic dose. In comparison to previous analog-based impedance sensors used for bacteria growth analysis, digital counting of impedance-signal - positive (i.e. bacteria containing) versus negative (i.e. empty) chambers increases precision and linearity by circumventing the noisy electrical data in traditional differential amplitude-based/analog methods.

We hereby describe a prototype system capable of electrical impedance analysis for monitoring growth of populations of bacterium. We show that reduction of the culture volume to nanoliter volumes allows detection of metabolic activity of a single bacterium. This is because the sensitivity of each electrode sensor is improved as the small (nanoliter) culture volume above each sensor increases the effective concentration of bacterial metabolites (i.e., the small volume of the nanowell enables more effective/confined diffusion of the metabolites to the sensor electrode). Our data also demonstrate that digital electrical assays enable differentiation of antimicrobial resistant versus susceptible strains of bacteria.

Materials and methods

Design of the multiplexed impedance system

The electrical hardware system used to measure the complex impedance is comprised of five sections (Fig. 1). The electrode pairs, multiplexer, addressing control, impedance measurement and microcontroller. The system is entirely powered and controlled via a single USB cable and implemented on a dual-sided printed circuit board.

The disposable electrode pairs on a glass substrate are connected via a high density 204 pin Dual In-Line Memory Module (DIMM) socket. A 96-channel (48 pairs) multiplexer selects the pair to be measured (each electrode pair is measured sequentially so that the measurement of N chambers can be viewed as occurring in series and not in parallel). One channel is reserved for a calibration resistor installed on the electrode substrate allowing de-embedding of the signal measurement path to the sensor.

Once the selected channel is active, the complex impedance can be measured. This is accomplished by applying a DDS (Direct Digital Synthesis) generated low level signal to the sensor electrodes and digitizing the resulting current vector. A discrete Fourier transform produces the real and imaginary components. The impedance is the ratio of the applied voltage and resulting vector current. The sinusoidal signal frequency is swept from 1 to 100 kHz, in steps to obtain spectral information from the sensor. The Analog Devices AD5933 integrated circuit is used for the impedance instrumentation. The selection of the multiplexer device is critical to making accurate measurements, and a low capacitance device Analog Devices ADG1207 was used. A DC-to-DC boost converter was required to provide the higher voltage needed by this multiplexer.

The multiplexer control is generated by a dual 8-bit shift-register, providing both addressing and enabling functions. The ARM-based microcontroller is responsible to interface the instrument to a PC, via the USB cable. This interface involves receiving commands, parsing the requests, calibrating the instrument, generating the multiplexer control, performing the measurement sweeps, and reporting the de-embedded test results. The reported data are then logged and plotted by a pc application software written in java-based "Processing" software.

Additional controls were designed into the circuit board to enable micro-fluidic automation via optically isolated driver channels; this would allow for actuation of pressure sources and fluidic valves for automated loading of samples/tests.

Electrode and sensor fabrication

The electrical sensors used to detect bacterial metabolic activity were constructed with standard wafer lithography processing techniques. Each electrical sensor consists of a pair of interdigitated electrodes, each addressed by a lead which terminates at a probe pad. A fused silica substrate was chosen (CoreSix Precision Glass, Williamsburg, VA), because it satisfied two critical aspects. Specifically, the material allows minimal leakage of electrical current across charged electrodes under test, and it is optically clear, which enables additional inspection of bacteria growth via optical microscopy for validation of the impedance-based readout. Optical inspection also enables quality control of the electrode and sensor fabrication (e.g., it can identify electrodes that are misaligned to the nanowell which can then be excluded from analysis).

Initial experiments sought to evaluate optimal electrode size, spacing, and surface metallurgy (Fig. S11). 5, 10 and 20 μm interdigitated electrodes were constructed, and exposed surfaces of Au, Pt, and Au passivated with SiO2 were evaluated. Tests conducted on these materials and optional

form factors resulted in a down selection to gold 10 µm electrodes.

Metallization of the glass wafers was initiated by sputtering an adhesion layer of 250A TiW, and then 1000 Å Au (KDF 603 Sputtering System, Rockleigh, NJ). 1.5 µm of AZ1512 positive photoresist was spun on the wafer (AZ Electronic Materials, Branchburg, NJ) (TEL Mark-5 Resist Coater, Austin TX), and a mask-based contact aligner used to pattern the resist (MA6/BA6, Suss MicroTec, Garching, Germany). The Au layer was wet-etched in a bath consisting of 10% KI, 5% I_2, and 85% water for approximately 1.5 minutes, and then the TiW layer was wet-etched for approximately 1 minute, in a solution of 30% Hydrogen Peroxide and 70% water. An SiO_2 passivation layer was deposited through plasma enhanced chemical vapor deposition (Plasma Lab System 100, Oxford Instruments, Abingdon, UK). A 1.08 µm layer of AZ703 photoresist was deposited, exposed and developed. This step removed the resist in specific areas that would be exposed to a wet oxide etch. The SiO_2 layer was removed above interdigitated electrode regions, as well as contact pads. Finally, individual chips were diced from the wafer with a Tcar dicing saw (Thermocarbon, Casselberry, FL).

The culture chambers were made using polydimethylsiloxane (PDMS) because back-pressure loading of individual bacteria into dead-end chambers requires a gas-permeable culture chamber material. The PDMS culture chambers were made using a 3D printed mold (Protolabs, Maple Plain, MN) or a photoresist mold as described previously[11], aligned, and bonded to the electrode-on-glass chips using an oxygen plasma bond. Specifically, Harrick Plasma Cleaner PDC-001 was used to both clean and activate the surfaces of the PDMS culture device and underlying glass coverslip that the PDMS was adhered to. The plasma chamber was first pumped down using a mechanical vacuum pump; a valve was then opened to allow oxygen into the chamber. The medium (15 Watt) setting on the plasma cleaner was selected and a visual check was performed to ensure generation of oxygen plasma within the barrel. The glass and PDMS components were treated in the plasma together for 30 seconds. The parts were immediately removed, aligned under stereomicroscope, and pressed together. Upon completion of this initial bonding process, the devices were incubated at 70°C for at least one hour in an oven.

The dimensions of each culture chamber was 400 µm x 100 µm x 100 µm (length, width, height) so that each culture chamber volume was 4 nL. The need for nanoliter volumes is determined below in the results section. The particular dimensions used to achieve our nanoliter volume was based on fabrication considerations.

Impedance data analysis for hand-held device

We analyzed the impedance spectra to determine the optimal impedance measurement parameter and frequency range for analysis (Fig. S2). We observed that bacterium growth may be monitored using the magnitude of the impedance, |Z|, or alternatively, it's real component, Z'. There is also a relatively wide range of frequencies suitable for monitoring. Although there is a wide range of frequencies suitable for monitoring, for the purpose of consistency in this initial report, all impedance data reported herein is summarized at 10 kHz.

The impedance data files generated were analyzed using custom software written in Python. The generated data files were read sequentially and converted into a tabular form that contained a time series of the impedance data generated during the duration of the experiment. Occasionally, there are wells that contained electronic noise due to incomplete electrical contact. To identify these outliers, we set two criteria. First, we labelled a well as an outlier if it experienced a positive impedance change during growth (instead of a negative change). Second, we labeled a well as an outlier if it experienced >10% change in impedance between subsequent measurements. These two rules consistently identified wells with electrical contact issues, and no further processing of the impedance data was needed.

To identify growth chambers, we determined a detection threshold from a series of 5 broth-only control samples that contained a total of 106 wells (these control samples contained broth and no bacteria). We set the detection threshold at 3 standard deviations from the mean of this control distribution (-31.4 percentage change). Wells that exceeded this threshold were classified as bacterium containing, and wells below this threshold were classified as non-bacterium containing. Due to evaporation, there is a random drift component that is included in the background value.

Bacteria culture and spiking experiments, estimation of Poisson loading ratio and device filling.

Bacterial strains were obtained from American Type Culture Collection (ATCC). *E. coli* strains ATCC 25922 (ampicillin-sensitive) or ATCC 35218 (TEM-1 plasmid-borne β-lactamase, ampicillin-resistant) were maintained in Tryptic Soy (TS) liquid broth or on Tryptic Soy agar plates. *Staphylococcus* strain ATCC 35984 (*S. epidermidis*, methicillin/multidrug-resistant) was maintained in a similar manner. *Mycobacterium bacteremicum* ATCC 25791 was cultured on Middlebrook 7H10 agar with OADC enrichment. A Keio *E. coli* knockout strain (*ilvD*::KAN) was obtained from Horizon Discovery Ltd as a proxy kanamycin-resistant strain. *E. coli* 137 was a clinical isolate.

For antibiotic susceptibility testing, strains were sub-cultured in cation-adjusted Mueller-Hinton broth (CAMHB) or TS broth. CAMHB was preferred due to comparatively lower conductivity (Fig. S3) in addition to being a consensus laboratory standard for MIC testing. The fastidious *M. bacteremicum* strain was sub-cultured in CAMHB supplemented with 3% lysed horse blood (LHB). Antibiotic compounds were purchased from Sigma, and concentrated solutions were prepared fresh for each experiment.

On the day of experiment, colonies from fresh isolates (streaked from -80˚C stocks) were transferred into rich broth, cultured at 37°C with agitation to mid-log phase, and culture turbidity was measured at 600 nm (A_{600}). Cells were then diluted to a desired concentration for either bulk or nanoliter

culture with or without antibiotics. For bulk culture, cells were generally diluted to ~1 x 10^8 cells/mL in order to observe robust conductivity changes within a couple doubling times (generally corresponding to ~1 A_{600} growth, or approximately 1 CFU per pL). For single-cell nanowell culture, bacteria were generally diluted in fresh TSB or CAMBH to 1 x 10^6 cells/mL which mathematically equates to approximately 4 CFU/4 nL (to load at least 1 CFU per chamber). Experimentally, we observed a Poisson loading ratio of 0.8 with this concentration (i.e. ~80% expected chambers containing at least one bacterium). Cell stock concentrations were estimated from A_{600} turbidity using a modified McFarland standard equation:

$$y = 29.857 x^3 - 9.8803 x^2 + 10.35 x + 0.5238$$

where y = cell number (in 10^8/mL units) and x = A_{600}. Accuracy of these cell estimates were evaluated by viability plating and visual microscopic enumeration of cells within nanoliter culture chambers.

Loading of bacteria into digital or nanoliter culture chambers was performed as described previously[11] using a needle-tipped syringe containing bacteria solutions to inject into the microfluidic array. A syringe pump was used to load sample and digitization oil into the device. Sample and oil was loaded into 1 mL syringes; sample was pumped into the devices at 10-20 microliters per minute flow rates until all chambers were filled (filling was monitoring using optical analysis under the microscope). Oil was then pumped into the device for digitization at 20-40 microliters per minutes, until all chambers were digitized.

During experiments, the nanoliter array was placed on a temperature-controlled microscope stage at 37°C. The bacteria were allowed to grow for two hours, and during electrical measurements, as described above. Gas/oxygen requirements for aerobic growth were maintained by diffusion across the thin PMDS walls of the device. The design of the chambers to achieve adequate gas diffusion is discussed below; in modelling cell growth in nanolitre chambers section.

Correlation of nanoliter culture impedance to bulk-scale culture conductivity

Bacteria were inoculated from a fresh stock plates into triplicate tubes of 10 ml rich broth and grown at 37°C with agitation to early-log phase. Cell numbers were estimated by A_{600} turbidity using McFarland standard equation, and each culture was diluted into 20 ml fresh medium to obtain starting concentrations as indicated in the figures, with or without antibiotics. These cultures were then incubated at 37°C with agitation at 250 rpm.

Upon inoculation and at regular intervals over the first 4 hours of outgrowth, one millilitre of sample was withdrawn from each culture, chilled on ice, and immediately centrifuged for 5 minutes at 15,000 x g at 5°C to pellet and remove bacteria. Eight hundred microliters of the cell-free supernatant were collected into 1.5 or 2 ml microcentrifuge tubes and chilled to -80°C for storage during the course of the experiment. In parallel, culture density was measured via A_{600} turbidity. To measure the recovery of bulk conductivity in fresh media (after spent media was exchanged with fresh media and the bacteria were allowed to continue growing/doubling), cells grown to ~ 1 A_{600} were centrifuged to remove spent media and the cell pellet was resuspended in fresh media for culture outgrowth and sample collection at regular intervals. One to four days after freezing, cell-free media supernatant samples were thawed and equilibrated to room temperature, and conductivity was measured using a Mettler-Toledo Seven Compact meter. The average of triplicate readings made for each sample is presented (CV < 0.2%).

Optical analysis of microfluidic culture arrays

To evaluate the growth of bacteria in microfluidic channels, bacterial growth rates were also measured optically using bright-field microscopy. The bacteria sample was loaded into the nanoliter array, which was then placed on a temperature-controlled microscope stage at 37°C. The bacteria were allowed to grow for two hours, and each well was imaged at regular time intervals. Cells were counted manually using these images. Wells containing more than one bacterium at zero hours were normalized by dividing the following counts by the "zero-hour" count. To perform AST, an antimicrobial drug was added to the sample and the growth was recorded in the same way. To determine the minimum inhibitory concentration (MIC), the drug concentration was reduced by a factor of two or four until the growth rate matched the control case, for which there was no drug added. The lowest drug concentration that resulted in no growth was taken as the MIC. Starting bacteria concentrations were determined by optical density at a wavelength of 600 nm using a NanoDrop 2000 (Thermo Scientific). Unless otherwise specified, serial dilutions were performed to reach a sample concentration of 5 $\times 10^5$ CFU/mL.

Modelling cell growth in nanoliter chambers

A numerical simulation was performed to study the bacterial growth in the nanoliter chamber (Fig. S4). This simulation (Comsol) estimated the oxygen concentration in the microfluidic device, which is a critical factor limiting the growth of aerobic bacteria. The 3D chamber was first simplified to a 2D model. The model comprised three PDMS-liquid interfaces and one liquid-glass interface. The initial concentration was $0.3125\ \mathrm{mol/m^3}$ and was gradually consumed by the bacteria. The oxygen consumption rate of an individual bacterium was approximated to be $1.78 \times 10^{-18}\ \mathrm{mol/(cell \cdot s)}$ and the diffusion coefficient was $2.1 \times 10^{-9}\ \mathrm{m^2/s}$. In addition, oxygen diffused through the PDMS-liquid interfaces to the medium. The influx rate was calculated using the Fick's first law.[28,29] In this case, the influx rate depends on the oxygen concentration gradient across the PDMS layer. The oxygen concentrations in different chambers were calculated for different bacteria concentrations. For small chambers with a large surface to volume ratio, the oxygen is sufficient to support bacterial growth at concentration as high as $1 \times 10^9\ \mathrm{CFU/mL}$.

$$Influx = D \cdot \Delta C / \Delta Z$$

D is the diffusivity of O_2 in PDMS (4.1×10^{-9} m^2/s), $\Delta \boldsymbol{C}$ is the O_2 concentration difference through the PDMS layer ($0.2 - c_{o_2\ in\ medium}$ mol/m^3), and $\Delta \boldsymbol{Z}$ is the PDMS thickness (1 mm).

Results

Testing the hand-held multiplexed impedance sensor system

We developed a custom, hand-held digital impedance sensing system that integrates a culture cartridge with an electrical control system (Fig. 1a and Fig. S1). The microfluidic culture cartridge consists of nanoliter chambers with interdigitated electrodes for *in situ* sensing. The electrical control system is built based on the AD5933 on-board impedance converter and network analyser (Analog Devices, Inc.) operating from 1 to 100 kHz. Connection to and sensing from arrays of nanoliter culture chambers is accomplished using a DIMM edge mount socket, which accepted a PDMS culture chamber array and enabled electrical connection of pairs of interdigitated sensing electrodes to a set of eight multiplexors that interfaced to a total of 50 culture chambers (unless otherwise specified). The multiplexors functioned as switches to sequentially address each set of sensing electrodes (that probe an individual culture chamber). A microcontroller was used to cycle through the multiplexors and obtain the complex impedance signal from each culture chamber, such that each nanowell was queried approximately once every 1.7 seconds (i.e., the entire culture cartridge with 50 nanowells was scanned every ~90 seconds).

We verified that the hand-held digital impedance sensing system matched the output from a bench top analyzer on both reference circuits (Fig. 1b) and the nanoliter chambers loaded with broth only (Fig. S1d,e). To assess impact of sample on stability of the impedance signal, we monitored the impedance from a control array that contained broth but no bacteria. We typically observed a measurable decrease in impedance over time, which was attributed to a small amount of evaporation taking place within the nanoliter chambers (Fig. S5 a,b). To minimize evaporation to <200 pL/hour from each chamber within the array, we minimized the thickness of the device (i.e., the volume of PDMS in the device that may hold water vapor), flooded a polymer jacket built above the device with water or broth to achieve high humidity. After these design changes, the maximum change in impedance (+/- 3 standard deviations) over a two-hour culture period was determined on 5 different devices (on 5 different days) and used as the baseline value for subsequent experiments (Fig. S5c). The baseline was utilized to threshold all bacteria growth experiments performed, and the value served the same purpose as background fluorescence values obtained in optical digital PCR systems.[30]

In addition to impedance sensing, the hand-held system was designed to automate sample loading. The microcontroller has the ability to drive a peristaltic fluidic pump and valve, in order to provide a positive pressure source to load the nanoliter culture array with sample. Temperature control was provided by placing the culture chamber array on a flat-bed PCR temperature cycler (set to constant 37°C). A temperature sensor was built into the array, calibrated prior to culture, and used to continuously monitor temperature. The microcontroller transmitted impedance and temperature data to a laptop via USB connection during culture, and the user controlled the system through a custom graphical user interface.

Estimation of culture volume needed for single cell analysis

To determine the culture volume needed to achieve limit of detection of 1 bacterium through concentration of metabolites, we developed a model system based on bulk-scale media conductivity and used it to assess impact of culture volume on limit of detection (Fig. 2). In these model experiments, increasing concentrations of *E. coli* from 10^5 to 10^8 CFU/mL were cultured for 0 to 240 minutes in standard culture tubes. At each time-point, an aliquot was taken from the sample and the bacteria were removed through centrifugation. The conductivity of cell-depleted media was then analyzed using a commercial small volume conductivity meter. Using this technique, the contribution of growth metabolites was assessed independently from cell presence (i.e., the bacteria were removed from the culture through centrifugation, but the metabolites remained). This method provided a model system for measuring the time required for bacteria metabolism to produce a detectable conductivity change within a defined volume range. For example, the bulk starting concentration of 10^5 CFU/mL had on average one bacterium in every 10 nanoliters of culture broth, while 10^8 CFU had one bacterium per 0.01 nanoliters of culture broth. As expected, the time required to produce a detectable conductivity change through metabolic activity was dependent on the starting concentration of bacteria (and thus the amount of culture volume per bacterium). The results indicated that to achieve a detectable conductivity change in bulk media, the nanowell array should be designed with relative chamber sizes of less than 10 nanoliters (Fig. 2).

In addition to these experiments, we also utilized a finite element model (Comsol®) to examine the effect of culture chamber size and bacteria concentration on oxygen flux and concentration within the nanowells (Fig. S4). We calculated that for the bacteria concentration range utilized herein (i.e. 1 bacterium per nanoliter at time zero, or ~1x10^6 CFU/ml, to 1 bacterium per picoliter, or ~1x10^9 CFU/ml), there is no appreciable decrease in oxygen concentration within the nanowells. This expected result confirmed that bacteria experience suitable environmental conditions for normal growth and replication rates in nanowell culture chambers.

Digital dilution and single cell analysis

The impedance spectrum from a sample containing a digital dilution of *E. coli* loaded to at least 1 CFU/chamber showed a substantial decrease in impedance relative to the control sample using our multiplexed system (Fig. 3a,b). After 120 minutes of culture time, the percentage change in impedance

at 10 kHz showed two distinct distributions with 91% of chambers crossing the threshold for positive detection (Fig. 3c-e). As expected from our preliminary bulk-scale conductivity and optical nanoliter growth tests (Fig. 2), compartmentalization of *E. coli* within the nanoliter chambers of the multiplexed impedance system enabled significant separation of the impedance signal between the bacteria-containing and empty chambers in short culture periods (e.g., 120 minutes total culture time). The negative impedance change would be expected due to rapid accumulation of metabolites in the nanowell environment, consistent with the conductivity change of cell-depleted media for bulk-scale growth (Fig. 2, also see Fig. S9 and Fig. S10). To our knowledge, this represents the first demonstration of a digital dilution and single cell analysis using an impedance-based sensing system.

Antibiotic susceptibility testing

We next investigated if impedance-based sensing could be used to distinguish antibiotic susceptibility in real-time, analogous to optical-based assays. For these studies, we first optically monitored digital growth rates of *E. coli* in nanowell culture arrays in the presence of antibiotic (i.e. ampicillin) relative to nanowell cultures in the absence of drug (Fig. 4). These results visually confirmed a minimum inhibitory concentration (MIC) for ampicillin at 2-8 µg/mL by nanowell culture, consistent with the quality control range for this strain (ATCC 25922). We next collected cell-depleted media to investigate conductivity changes during bulk-scale growth in the presence or absence of antibiotic (i.e. ampicillin or doxycycline). These bulk-scale measurements confirmed conductivity changes within ~1 hr of drug introduction relative to no-drug controls (Fig. S6), thus confirming feasibility for monitoring *E. coli* susceptibility via electrical conductivity.

To further extend upon these results for digital monitoring in the presence and absence of antibiotics, we next utilized a bench top impedance analyzer (Keysight E4990A) to corroborate that antibiotic susceptibility can be manually discriminated in individual nanowells, and that growth inhibition by antimicrobial drugs leads to a detectable digital impedance signature. Fig. 5 summarizes results from digital *E coli* experiments in which nanowell chambers were loaded at digital bacterial concentrations with either susceptible or resistant strains. End-point impedance changes from each nanowell that are different than baseline (as measured from empty control chambers) are depicted within orange-shaded regions (i.e. “culture positive” detection). Representative control growth in the absence of drug (Fig. 5b) showed ~81% culture-positive chambers (Fig. 5b), in agreement with the expected 0.8 Poisson loading ratio. Incubation of this strain in the presence of ampicillin or kanamycin resulted in a decrease of growth-positive chambers to 40% or 28%, respectively (Fig. 5c-d). In contrast, incubation of two different resistant strains with the same antibiotics (Fig. 5e-f) demonstrated little change in culture-positive chambers. Similar media conductivity changes were detectable during bulk-scale growth (Fig. S8). This evidence further validates the use of multiplexed digital impedance assays to determine bacteria susceptibility to antibiotics.

Finally, we extended our nanowell growth analysis to slower-growing Gram-positive (*S. epidermidis*) and acid-fast fastidious (*M. bacteremicum*) species. Relative to *E. coli*, we confirmed longer culture times are required for both optical and electrical detection of growth (Fig. S7). The slower rate change in conductivity observed among these strains will necessitate longer impedance monitoring timeframes (i.e. ≥2.5 hrs) for nanowells. Further device optimization will be required to support longer continuous impedance monitoring of slower-growing strains, such as further reducing chamber size dimensions or fabricating with non-PDMS materials to avoid sample evaporation issues.

Discussion

To our knowledge, our results show the first impedance-based readout of digital culture arrays to monitor bacterial growth and antimicrobial susceptibility. As such, this report demonstrates that electrical sensing systems might provide compact, hand-held, and lower-cost alternatives to the current optical-based systems[9,11,14,16,18] used for digital or single cell analysis. In addition, the decreased ratio of culture volume-to-sensor within the arrays (i.e. approximately four nanoliters of culture volume per sensor) enable rapid metabolic growth sensing (i.e. less than one-hour detection for single *E. coli*). The time scales associated with this electrical readout is consistent with those recently found in optical-based single bacteria sensing platforms[9,11,16] and represents a clear improvement to current bulk culture methods for AST.[12,22] We demonstrate AST detection times for single *E. coli* within 1-3 cell doublings (i.e. < 1hr), although data from slower-growing species indicate that cell growth is rate-limiting for electrical conductivity assessment. We believe reductions in detection time are achievable by further miniaturizing the culture chambers, which might be reduced by another order of magnitude (i.e. 10-micron side walls, enabling picoliter chamber volumes) before encountering challenges with cell loading, culturing, and sensing. Finally, the scalability of our approach through multiplexing makes it a suitable solution for addressing rapid AST needs for point-of-care diagnostic applications, although certain limitations exist. For example, filling each nanowell currently involves passive Poisson-based efficiency and therefore high concentrations of input bacteria ($\geq 10^6$/mL) are required, consistent with other microfluidic devices.[30,31] Developing and integrating upstream sample prep for concentrating bacteria into small volumes may improve nanowell utility, such as potential applications for direct-from-blood AST. Growth mediums for AST also possess different electrical baselines (Fig. S3) so certain drugs normally tested with extra media salts or cations (for example, oxacillin or daptomycin) could also affect signal-to-noise ratios during electrical monitoring.

This study captures initial electrical patterns of metabolism that could be important for future work on digital impedance systems. First, it appears that bacterial metabolism in the

presence of antibiotics is not zero within the first hours of culture. It is currently not well known how the biochemical mechanisms of different drugs affects the timeline of metabolism (within the first one or two double times). Different modes of inhibiting bacterial growth (i.e. bacteriostatic drugs like doxycycline vs. bactericidal drugs like ampicillin and kanamycin) could result in distinguishable electrical signatures, perhaps also in a concentration-dependent manner. Future studies should investigate possibilities for differentiating between antimicrobials/mode of action using real-time impedance measurements with single cells. It is also noteworthy that AST within polymicrobial samples typically requires lengthy pre-culture steps, in order to isolate each unique species/strain prior to drug resistance testing. In the future, digital impedance-based sensing may enable direct readout of drug-induced growth-rate/impedance signatures from individual bacterium in mixed populations that include both drug susceptible and drug resistant, or pathogenic and commensal bacteria.

The impedance sensing and multiplexing circuit we described herein is modular and easily expandable (i.e. the circuit is simply replicated and each unit enables sensing from at least 50 additional culture chambers). In addition, the culture chamber array can be modified and scaled using alternative electrode manufacturing techniques in the future. Specifically, the electrical traces and sensors can be fabricated using current printed circuit board technologies (PCB)[32], which are capable of multi-layer and low-cost construction. Using multi-layer construction, impedance sensing chambers could be built with closer proximity to each other (i.e. 100's of microns) by running electric connections from each electrode pair to the sensing circuits within sub-layers beneath the culture surface. In future reports, we will use these fabrication technologies to build electrical digital sensing platforms that match the chamber density (i.e. 1000's of culture chambers per device) and dynamic range of optical platforms (that have developed from the original 100s chambers reports[32] to over 10,000 today[34]). The data herein, represents the initial steps toward new (non-optical) capabilities for digital and single-cell sensing, with less complex and lower-cost integrated electrical sensing components that should advance clinical applications such as AST.

Conclusions

We have developed a novel electrical impedance based digital platform to monitor single cell metabolism, and rapidly detect the growth and assess the antimicrobial susceptibility of different species of bacteria. The microfluidic nature of this sensing platform greatly improves its detection sensitivity over the conventional methods, and the compact format and cost-efficient construction of the electrical analyzer further improves its utility over the bulky optical platforms. The scalability and multiplexing format of this handheld system enable high throughput digital testing, thus making it a potential platform for diagnostic applications toward combatting the crisis of antimicrobial resistance.

Author contributions

C.P. secured the funding and administered the project. J.R.N, R.A.P., P.K.W., T.H.W., and C.P. conceptualized research goals and supervised research activities. Experiments were designed, completed and analyzed by B.S., C.S., E.K., C.G., S.G., R.S., C.P., H.L., P.T., G.G., T.H., T.J. and W.H. The paper was written by B.S., E.K., C.S., T.K., and C.P.

Conflicts of interest

Some authors are employees of GE and GE has submitted a patent application on digital impedance detection and analysis of AST.

Acknowledgements

Portions of this research or manuscript completion were developed with funding from the Defense Threat Reduction Agency (DTRA; HDTRA1-16-C-0004 30 or MCDC-18-01-01-012). The views, opinions and/or findings expressed are those of the author and should not be interpreted as representing the official views or policies of the Department of Defense or the U.S. Government.

References

1 E. A. Idelevich and K. Becker, *Clinical Microbiology and Infection*, 2019, **25**, 1347–1355.
2 N. R. Naylor, N. Zhu, M. Hulscher, A. Holmes, R. Ahmad and J. V. Robotham, *Clinical Microbiology and Infection*, 2017, **23**, 806–811.
3 N. Friedman, *Antibiotics*, 2013, **2**, 400–418.
4 L. S. J. Roope, R. D. Smith, K. B. Pouwels, J. Buchanan, L. Abel, P. Eibich, C. C. Butler, P. S. Tan, A. S. Walker, J. V. Robotham and S. Wordsworth, *Science*, 2019, **364**, eaau4679.
5 A. van Belkum and W. M. Dunne, *Journal of Clinical Microbiology*, 2013, **51**, 2018–2024.
6 A. van Belkum, T. T. Bachmann, G. Lüdke, J. G. Lisby, G. Kahlmeter, A. Mohess, K. Becker, J. P. Hays, N. Woodford, K. Mitsakakis, J. Moran-Gilad, J. Vila, H. Peter, J. H. Rex and W. M. Dunne, *Nat Rev Microbiol*, 2019, **17**, 51–62.
7 M. Davenport, K. E. Mach, L. M. D. Shortliffe, N. Banaei, T.-H. Wang and J. C. Liao, *Nat Rev Urol*, 2017, **14**, 296–310.
8 P. Athamanolap, K. Hsieh, L. Chen, S. Yang and T.-H. Wang, *Anal. Chem.*, 2017, **89**, 11529–11536.
9 C. Surrette, B. Scherer, A. Corwin, G. Grossmann, A. M. Kaushik, K. Hsieh, P. Zhang, J. C. Liao, P. K. Wong, T. H. Wang and C. M. Puleo, *SLAS TECHNOLOGY: Translating Life Sciences Innovation*, 2018, **23**, 387–394.
10 A. M. Kaushik, K. Hsieh, L. Chen, D. J. Shin, J. C. Liao and T.-H. Wang, *Biosensors and Bioelectronics*, 2017, **97**, 260–266.
11 K. Hsieh, H. C. Zec, L. Chen, A. M. Kaushik, K. E. Mach, J. C. Liao and T.-H. Wang, *Anal. Chem.*, 2018, **90**, 9449–9456.
12 S. O. Kelley, SLAS TECHNOLOGY: Translating Life Sciences Innovation, 2017, **22**, 113–121.
13 N. G. Schoepp, T. S. Schlappi, M. S. Curtis, S. S. Butkovich, S. Miller, R. M. Humphries and R. F. Ismagilov, *Sci. Transl. Med.*, 2017, **9**, eaal3693.
14 N. G. Schoepp, E. M. Khorosheva, T. S. Schlappi, M. S. Curtis, R. M. Humphries, J. A. Hindler and R. F. Ismagilov, *Angew. Chem. Int. Ed.*, 2016, **55**, 9557–9561.

15 T. Khazaei, J. T. Barlow, N. G. Schoepp and R. F. Ismagilov, *Sci Rep*, 2018, **8**, 11606.
16 N. Cermak, S. Olcum, F. F. Delgado, S. C. Wasserman, K. R. Payer, M. A. Murakami, S. M. Knudsen, R. J. Kimmerling, M. M. Stevens, Y. Kikuchi, A. Sandikci, M. Ogawa, V. Agache, F. Baléras, D. M. Weinstock and S. R. Manalis, *Nature Biotechnology*, 2016, **34**, 1052–1059.
17 P. Athamanolap, K. Hsieh, C. M. O'Keefe, Y. Zhang, S. Yang and T.-H. Wang, *Anal. Chem.*, 2019, **91**, 12784–12792.
18 J. Choi, J. Yoo, M. Lee, E.-G. Kim, J. S. Lee, S. Lee, S. Joo, S. H. Song, E.-C. Kim, J. C. Lee, H. C. Kim, Y.-G. Jung and S. Kwon, *Science Translational Medicine*, 2014, **6**, 267ra174-267ra174.
19 Rapid Automatic Bacterial Impedance Technique (RABIT), Don Whitley Scientific, https://www.dwscientific.com/rapid-methods/rabit, (accessed November 2020).
20 BacTrac 4300 Microbiological Impedance Analyzer, Sylab, https://microbiology.sylab.com/products/p/show/Product/product/bactrac-4300.html, (assessed November 2020).
21 M. Grossi, R. Lazzarini, M. Lanzoni, A. Pompei, D. Matteuzzi and B. Ricco, *IEEE Sensors J.*, 2013, **13**, 1775–1782.
22 X. Muñoz-Berbel, N. Godino, O. Laczka, E. Baldrich, F. X. Muñoz and F. J. del Campo, in *Principles of Bacterial Detection: Biosensors, Recognition Receptors and Microsystems*, eds. M. Zourob, S. Elwary and A. Turner, Springer New York, New York, NY, 2008, pp. 341–376.
23 R. Gomez-Sjoberg, D. T. Morisette and R. Bashir, *J. Microelectromech. Syst.*, 2005, **14**, 829–838.
24 D. Butler, N. Goel, L. Goodnight, S. Tadigadapa and A. Ebrahimi, *Biosensors and Bioelectronics*, 2019, **129**, 269–276.
25 S. Sengupta, D. A. Battigelli and H.-C. Chang, *Lab Chip*, 2006, **6**, 682.
26 L. Yang and R. Bashir, *Biotechnology Advances*, 2008, **26**, 135–150.
27 R. A. Potyrailo, J. Dieringer, V. Cotero, Y. Lee, S. Go, M. Schulmerich, G. Malmquist, A. Castan, K. Gebauer and V. Pizzi, *Bioelectrochemistry*, 2019, **125**, 97–104.
28 C. H. Chen, Y. Lu, M. L. Y. Sin, K. E. Mach, D. D. Zhang, V. Gau, J. C. Liao and P. K. Wong, *Anal. Chem.*, 2010, **82**, 1012–1019.
29 E. Leclerc, Y. Sakai and T. Fujii, *Biomedical Microdevices*, 2003, **5**, 109–114.
30 H. Li, P. Torab, K. E. Mach, C. Surrette, M. R. England, D. W. Craft, N. J. Thomas, J. C. Liao, C. Puleo and P. K. Wong, *Proc Natl Acad Sci USA*, 2019, **116**, 10270–10279.
31 Ö. Baltekin, A. Boucharin, E. Tano, D. I. Andersson and J. Elf, *PNAS*, 2017, **114**, 9170–9175.
32 J. Gong and C. Kim, Journal of Microelectromechanical Systems, 2008, **17**, 257–264.
33 B. Vogelstein and K. W. Kinzler, *PNAS*, 1999, **96**, 9236–9241.
34 A. S. Basu, SLAS TECHNOLOGY: Translating Life Sciences Innovation, 2017, **22**, 369–386.

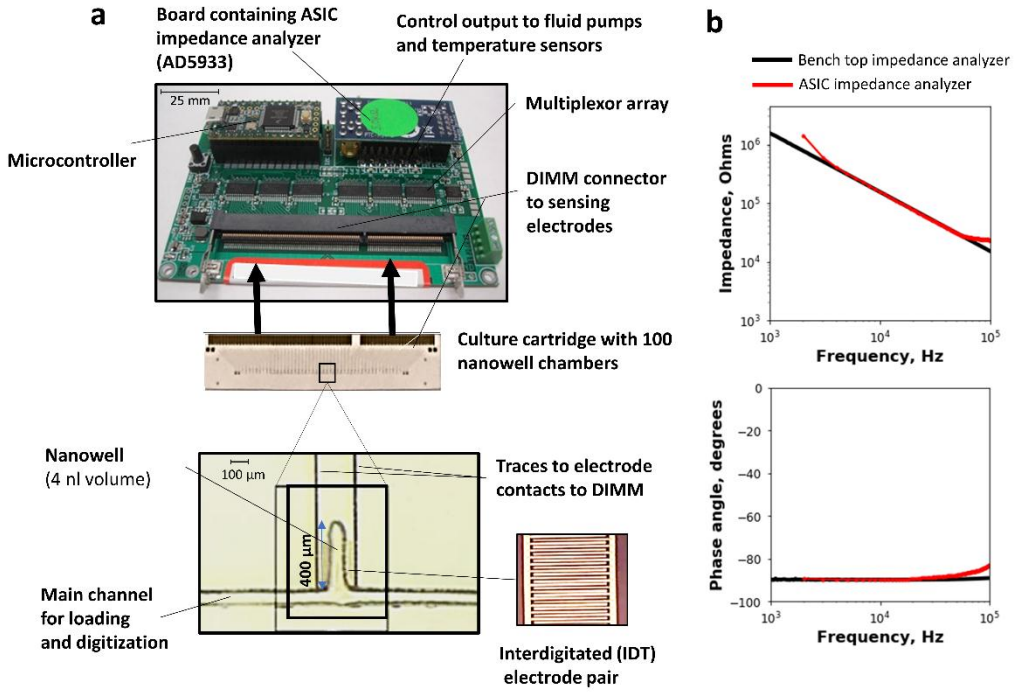

Fig. 1 Overview of the multiplexed impedance system. (a) The array of nanowell culture chambers are fabricated on a glass slide containing a SODIMM socket, which enables a "plug-and-play" interface to the multiplex, electrical impedance system. After bacteria are loaded at low concentrations (<1 CFU/chamber) for digital analysis, a multiplexor and ASIC impedance analyzer chip (AD5933) measures the impedance from microfabricated interdigitated electrodes built at the bottom of a each nanowell. This system also contains a pump for automated sample loading. (b) Benchmark data showing the impedance measured on reference circuits matched the impedance measured on a bench top analyzer (Keysight E4990A). Additional benchmark data is shown in Fig. S1.

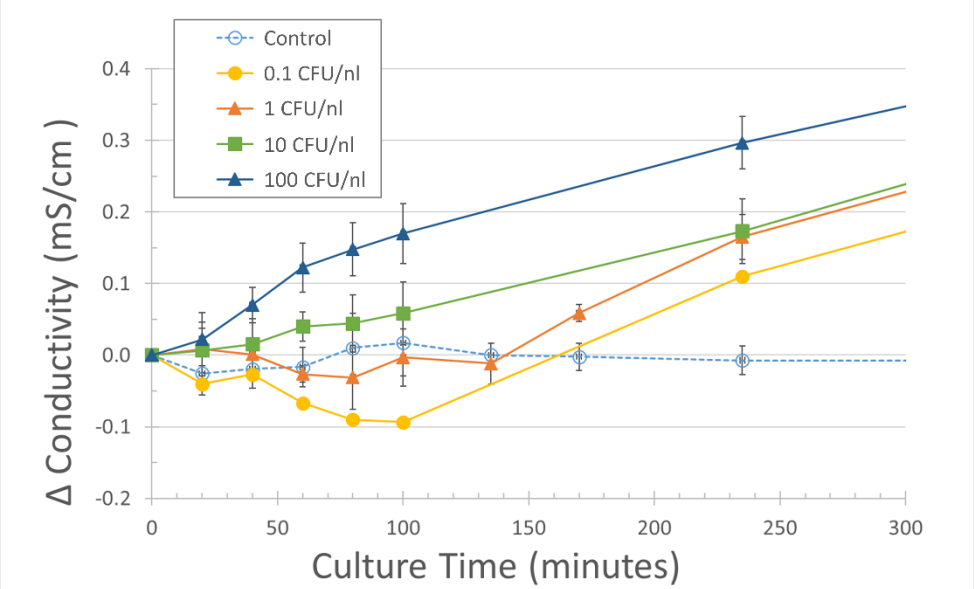

Fig. 2 The impact of culture density on detectable changes in media conductivity. The time required to produce a detectable conductivity change through metabolic activity was dependent on the starting concentration of bacteria (and thus the amount of culture volume per bacterium). *E. coli* (ATCC 25922) was grown to mid-log phase in rich medium (Tryptic Soy broth) and inoculated into 20 ml fresh medium to the indicated initial densities. Each growth condition was replicated in triplicate and measurements made in parallel. Aliquots of 1 ml were withdrawn at indicated times, immediately chilled on ice, and clarified by centrifugation at 12,000 x g for 5 min at 5°C , then flash-frozen to -80°C during collection (in order to enable simultaneous analysis of all sample collected during the course of the experiment). Conductivity of the cell-free media supernatant sample set was then measured at room temperature on a Mettler-Toledo Seven Compact meter.

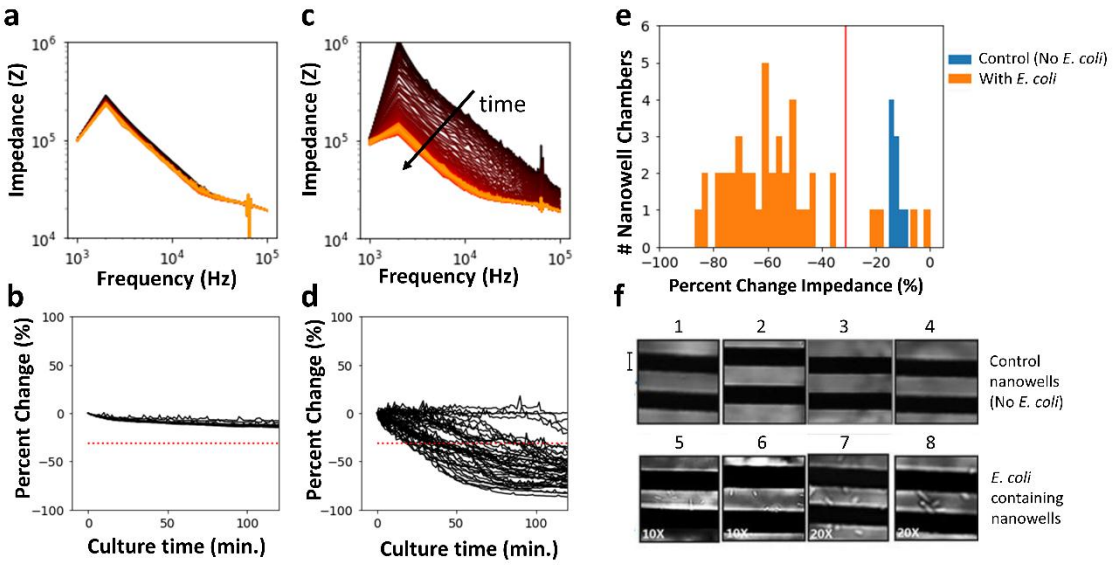

Fig. 3 Electrical impedance data measured during digital dilution and single cell analysis (1 CFU/chamber). The impedance spectra and percent change in impedance at 10 kHz are shown for nanowells filled with (a, b) media only and (c, d) *E. coli* in media. (e) The percent change in impedance between empty and *E. coli*-containing nanowells formed two distinct distributions. The red line in panels b, d, and e indicates the threshold used to determine the cut-off between culture positive and empty or culture negative chambers (this value is determined from multiple controls collected on multiple days, see Fig. S5). (f) Exemplary images showing a representative portion of eight nanowell culture chambers after growth incubation, with and without *E.* coli (wells 1-4 and 5-8, respectively). The black horizontal lines are the electrodes (the scale bar on image 1 represents 10 um).

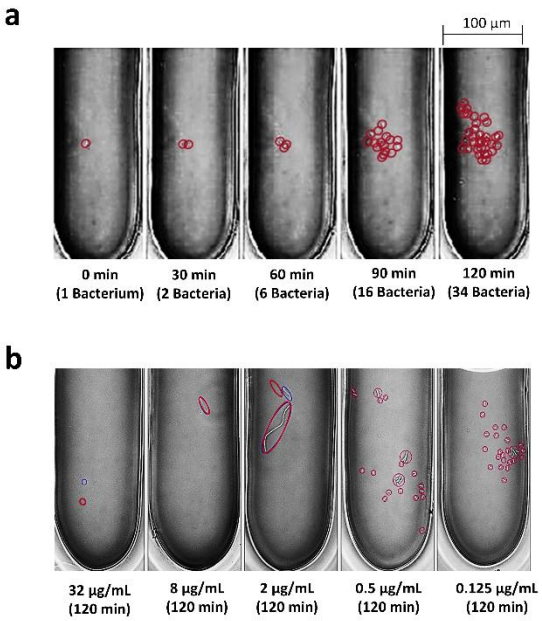

Fig. 4 Verification that nanowell culture does not inhibit bacteria growth, and enables detection of growth inhibition during growth in the presence of antimicrobials. (a) Optical microscopic images of *E. coli* growth in a single bacterium containing chamber over time; the circles outline the original bacterium and its progeny over the times lapse series of images. (b) Optical microscopic images of *E. coli* growth in a single bacterium containing chamber after 120 minutes of culture for multiple concentrations of ampicillin. Ampicillin inhibited growth throughout the expected concentrations (i.e. greater than the cited mean inhibitory concentration (MIC)); however, at lower concentrations of drug there was a short period of single bacteria lengthening (i.e. the contained bacteria gets longer without dividing) during culture. These drug specific biophysical effects at short culture times may contribute to impedance changes during growth in drug containing culture.

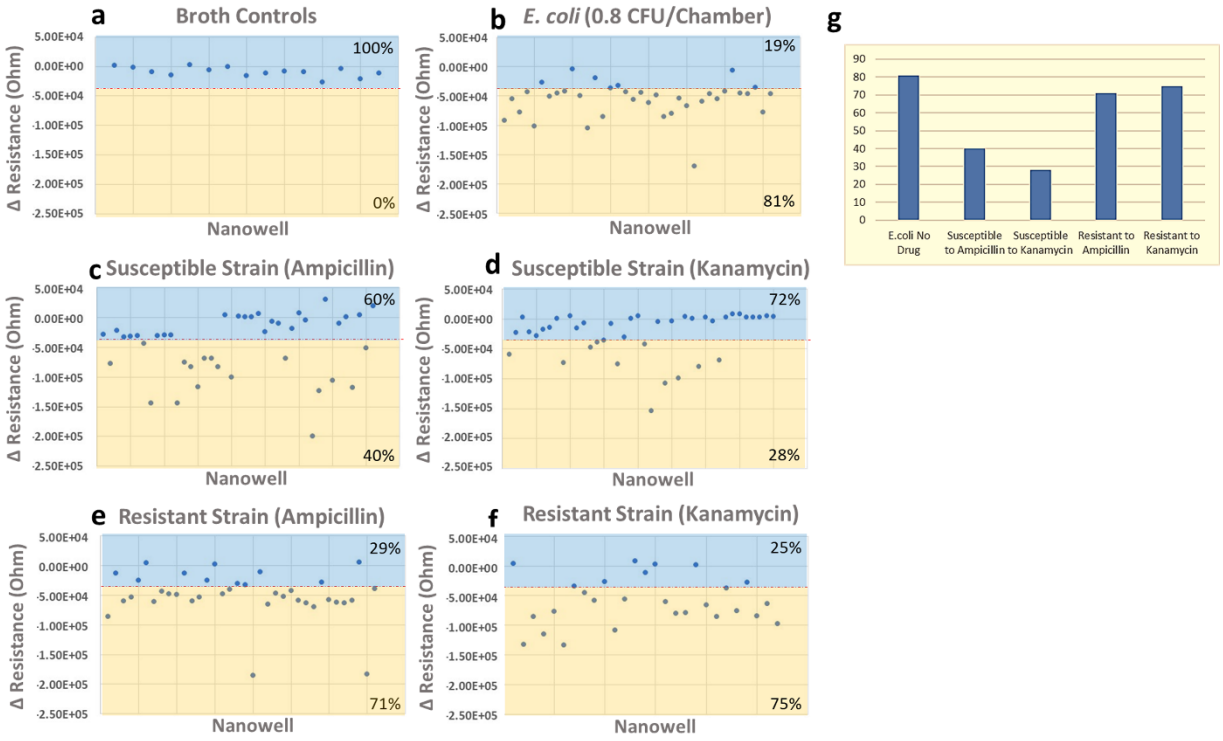

Fig. 5 Antimicrobial Susceptibility Testing using bench top impedance analyzer and 10-nanowell arrays. A total of 195 chambers were summarized from multiple experiments; of this grouping, 15 chambers contained broth alone to determine the baseline resistance change, while the remaining chambers (30-40 chambers/condition) contained either susceptible or resistant *E. coli* in standard culture broth or broth containing the MIC concentration of ampicillin or kanamycin. We measured the change in resistance over a 60 minutes incubation period. (a) The change in resistance for broth alone (no bacteria) indicated 100% chambers were growth negative (blue shaded region on the plots), and 0% were growth positive (red shaded region). (b) In chambers loaded with *E. coli* (0.8 CFU/chamber) but no drug, 81% of the chambers were growth positive, while 19% were growth negative. (c) Using a susceptible strain of *E. coli* (loaded at an equivalent 0.8 CFU/chamber) loaded in the presence of 100 µg/mL of ampicillin resulted in a reduction of chambers showing positive growth compared to the no drug controls. (d) Using a susceptible strain of *E. coli* (loaded at an equivalent 0.8 CFU/chamber) loaded in the presence of 50 µg/mL of kanamycin resulted in a reduction of chambers showing positive growth compared to the no drug controls (i.e., 28% positive and 72% negative chambers). (e) Culture of a drug resistant strain of *E. coli* (loaded at an equivalent 0.8 CFU/chamber) loaded in the presence of ampicillin resulted in a number of positive growth chambers that approached the no drug controls (i.e., 71% positive growth chambers versus the 81% in controls). (f) Culture of a drug resistant strain of *E. coli* (loaded at an equivalent 0.8 CFU/chamber) loaded in the presence of 50 µg/mL kanamycin resulted in a number of positive growth chambers that approached the no drug controls (i.e., 75% positive growth chambers versus the 81% in controls). (g) bar plot summarizing these results.